MTL TR 89-101

AD-A216 950

BIAXIAL STRENGTH AND STRESS RUPTURE OF HOT-PRESSED SILICON NITRIDE

GEORGE D. QUINN
U.S. ARMY MATERIALS TECHNOLOGY LABORATORY
CERAMICS RESEARCH BRANCH

GUNTER WIRTH
INSTITUT FUR WERKSTOFF - FORSCHUNG
FEDERAL REPUBLIC OF GERMANY

November 1989

US ARMY
LABORATORY COMMAND
MATERIALS TECHNOLOGY LABORATORY

U.S. ARMY MATERIALS TECHNOLOGY LABORATORY
Watertown, Massachusetts 02172-0001

UNCLASSIFIED

SECURITY CLASSIFICATION OF THIS PAGE *(When Data Entered)*

REPORT DOCUMENTATION PAGE		READ INSTRUCTIONS BEFORE COMPLETING FORM
1. REPORT NUMBER MTL TR 89-101	2. GOVT ACCESSION NO.	3. RECIPIENT'S CATALOG NUMBER
4. TITLE *(and Subtitle)* BIAXIAL STRENGTH AND STRESS RUPTURE OF HOT-PRESSED SILICON NITRIDE		5. TYPE OF REPORT & PERIOD COVERED Final Report 6. PERFORMING ORG. REPORT NUMBER
7. AUTHOR(s) George D. Quinn and Gunter Wirth*		8. CONTRACT OR GRANT NUMBER(s)
9. PERFORMING ORGANIZATION NAME AND ADDRESS U.S. Army Materials Technology Laboratory Watertown, Massachusetts 02172-0001 SLCMT-EMC		10. PROGRAM ELEMENT, PROJECT, TASK AREA & WORK UNIT NUMBERS D/A Project: 1L161105.AH84
11. CONTROLLING OFFICE NAME AND ADDRESS U.S. Army Laboratory Command 2800 Powder Mill Road Adelphi, Maryland 20783-1145		12. REPORT DATE November 1989 13. NUMBER OF PAGES 16
14. MONITORING AGENCY NAME & ADDRESS *(if different from Controlling Office)*		15. SECURITY CLASS. *(of this report)* Unclassified 15a. DECLASSIFICATION/DOWNGRADING SCHEDULE

16. DISTRIBUTION STATEMENT *(of this Report)*

Approved for public release; distribution unlimited.

17. DISTRIBUTION STATEMENT *(of the abstract entered in Block 20, if different from Report)*

18. SUPPLEMENTARY NOTES

*Institut fur Werkstoff - Forschung, DLR+, D 5000 Cologne, Federal Republic of Germany

19. KEY WORDS *(Continue on reverse side if necessary and identify by block number)*

Silicon nitride	Stress rupture testing
Static fatigue life	Fractography
Disk testing	Weibull analysis

20. ABSTRACT *(Continue on reverse side if necessary and identify by block number)*

(SEE REVERSE SIDE)

DD FORM 1 JAN 73 1473 EDITION OF 1 NOV 65 IS OBSOLETE

UNCLASSIFIED

SECURITY CLASSIFICATION OF THIS PAGE *(When Data Entered)*

Block No. 20

ABSTRACT

The equibiaxial static fatigue resistance of hot-pressed silicon nitride was measured at high temperature. A concentric ring scheme was used to load disks at up to 1300°C in air. Equibiaxial lifetimes were substantially shorter than uniaxial lifetimes, primarily a consequence of a drastically reduced biaxial strength. The static fatigue trends were similar in uniaxial and biaxial loading. The ring-on-ring scheme is not suitable for stress rupture testing if creep deformations are present or cracks grow large without going critical.

CONTENTS

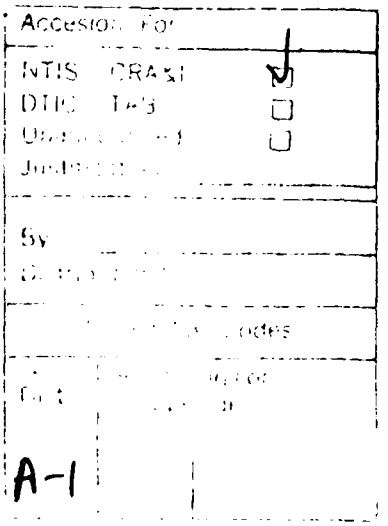

INTRODUCTION

Static fatigue failure of structural ceramics can be caused by a variety of phenomena including stress corrosion, slow crack growth, surface pit formation, and creep fracture.[1] Hot-pressed silicon nitride (HPSN) with magnesia sintering aid has been extensively studied due to its extremely consistent behavior.[2] Slow crack growth from preexisting flaws, or creep fracture, can control static fatigue in HPSN.[3-6] An extensive data base of flexural stress rupture experiments has culminated in a fracture mechanism map, ~~as shown in Figure 1.~~[3,4]

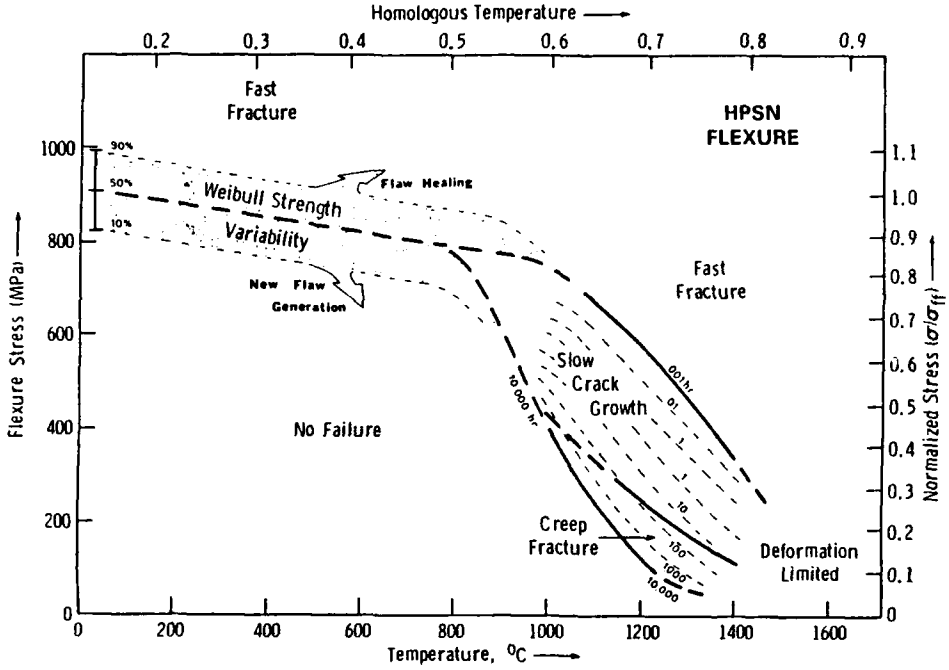

Figure 1. Flexure fracture mechanism map for HPSN, References 3 and 4.

The vast majority of static fatigue experiments for engineering ceramics have been in a uniaxial stress state, indeed, usually in four-point flexure. Two studies have compared uniaxial and biaxial slow crack growth for alumina, glass, and a glass ceramic,[7,8] and a vitreous-bonded abrasive.[9] Testing done was only at room temperature, and with short duration, dynamic fatigue experiments

1. QUINN, G. *Review of Static Fatigue in Silicon Nitride and Silicon Carbide.* Ceram. Eng. and Sci. Proc., v. 3, 1987, p. 77-98.
2. QUINN, G., and SWANK, L. *Static Fatigue of Preoxidized Hot Pressed Silicon Nitride.* Comm. Amer. Ceram. Soc., Febr ıry 1983, p. C31-C32.
3. QUINN, G. *Static Fatigue Resistance of Hot Pressed Silicon Nitride* in Fracture Mechanics of Ceramics, v. 8, R. Bradt, A. Evans, D. Hasselman, and F. Lange, ed., Plenum Press, New York, 1986, p. 319-332.
4. QUINN, G. *Fracture Mechanism Maps for Silicon Nitride.* Ceramic Materials and Components for Engines, Deutsche Keramische Gesellschaft, Berlin, 1987, p. 931-939.
5. GRATHWOHL, G. *Regimes of Creep and Slow Crack Growth in High Temperature Rupture of Hot Pressed Silicon Nitride* in Deformation of Ceramic Materials II, R. Tressler and R. Bradt ed., Plenum Press, New York, 1984, p. 513-587.
6. GRATHWOHL, G. *Creep and Fracture of Hot Pressed Silicon Nitride with Natural and Artificial Flaws* in Creep and Fracture of Engineering Materials and Structures, B. Wilshire and D. Owen, ed., Pineridge Press, Swansea, 1984, p. 565-577.
7. PLETKA, B., and WIEDERHORN, S. *A Comparison of Failure Predictions by Strength and Fracture Mechanics Techniques.* J. Mat. Sci., v. 17, 1982, p. 1247-1268.
8. PLETKA, B., and WIEDERHORN, S. *Subcritical Crack Growth in Glass Ceramics* in Fracture Mechanics of Ceramics, v. 4, R. Bradt, D. Hasselman, and F. Lange, ed., Plenum Press, New York, 1980, p. 745-759.
9. SERVICE, T., and RITTER, J. *Dynamic Fatigue of a Vitreous Bonded Abrasive Tested in Four Point and Ring-on-Ring Flexure.* Adv. Cer. Mat., v. 3, 1988, p. 49-51.

These studies were encouraging, however, showing that the multiaxial stress state had no effect upon crack growth parameters determined by strength test methods.

This study reports high temperature and long duration equibiaxial stress rupture experiments for HPSN. HPSN was chosen because of its high static fatigue reproducibility. It was also possible to examine more than one failure mechanism. The biaxial results are directly compared to comprehensive uniaxial results from References 3, 4, and 10. Biaxial testing was performed in both the slow crack growth and creep fracture regimes.

MATERIAL

The HPSN was NC 132 grade and was made in 1977.* This material has a magnesia sintering aid and has been previously characterized.[10,11] Disk specimens were cut from a single plate identified as billet L. This was made from the same powder lot and was pressed at the same time as billets A, C, and P described previously.[3,4] Strength limiting defects in this material are typically machining damage from surface grinding and tungsten carbide or disilicide inclusions.[11,12]

EXPERIMENTAL PROCEDURE

Thirty disks were prepared with 45 mm diameter and 2.2 mm thickness. The disks were prepared by conventional slicing and diamond grinding, but with special care to minimize machining damage in the final steps. The disks were then intended to be lapped very flat and to a depth of 25 μm from each side. The 25 μm is far greater than is necessary to produce a mirror finish and was designed to eliminate typical machining damage inherent to the grinding process. This machining damage is anisotropic[13] and, as such, would confound interpretation of biaxial effects on randomly dispersed flaws.

Seventeen flexure specimens of size 2.1 x 2.8 x 45 mm were prepared from the same billet in order to be broken at room temperature for a comparison of uniaxial to biaxial fast fracture strengths. The specimens were given the same grinding and lapping preparations as the disks. They were broken in accordance with MIL-STD-1942 (MR) four-point size B. The four-point spans were 40 x 20 mm and rollers permitted relief of friction constraint. (All other uniaxial and biaxial tests were under conditions where friction relief could not be assured.) The nonstandard specimen size was used to facilitate comparison of results to earlier data sets.[3,4,10]

These precautions were taken to ensure the strength limiting flaws were identical in uniaxial and biaxial specimens. Giovan and Sines[14] found such precautions necessary in their study of uniaxial and biaxial strengths of alumina.

*Norton Company, Worcester, MA, USA.

10. QUINN, G., and QUINN, J. *Slow Crack Growth in Hot Pressed Silicon Nitride* in Fracture Mechanics of Ceramics, v. 6, R. Bradt, A. Evans, D. Hasselman, and F. Lange, ed., Plenum Press, New York, 1983, p. 603-636.
11. QUINN, G. *Characterization of Turbine Ceramics after Long Term Environmental Exposure.* U.S. Army Materials Technology Laboratory, MTL TR 80-15, 1980.
12. BAUMGARTNER, H., and RICHERSON, D. *Inclusion Effects on the Strength of Hot Pressed Si_3N_4* in Fracture Mechanics of Ceramics, v. 1, R. Bradt, D. Hasselman, and F. Lange, ed., Plenum Press, New York, 1974, p. 367-386.
13. RICE, R. W., FREIMAN, S. W., MECHOLSKY, Jr., J. J., RICH, R., and HARADA, Y. *Fractography of Si_3N_4 and SiC* in Ceramics for High Performance Applications II, J. Burke, E. Lenoe, and R. Katz, ed., Brook Hill, Chestnut Hill, MA, 1978, p. 669-687.
14. GIOVAN, M. N., and SINES, G. *Biaxial and Uniaxial Data for Statistical Comparisons of a Ceramic's Strength.* J. Am. Ceram. Soc., v. 62, no. 9-10, 1979, p. 510-515.

The biaxial fixtures are shown schematically in Figure 2. Loading was via a ring-on-ring jig which produces an equibiaxial stress state. The rings were made from tubes of high purity recrystallized silicon carbide.* This material was chosen because of its high refractoriness and ready availability in tube form. Indeed, after all experiments, the appearance of the SiC had hardly changed and there was no chemical reaction evident at the load points. The top of each tube was crowned with a radius such that the support (outer) ring had a nominal diameter of 40 mm and the loading (inner) ring of 10 mm. A silicon nitride ball with a flat was used to apply the load centrally to the loading ring. The assemblage was aligned at room temperature and held in place by tack beads of a household acetate cement which subsequently burned off.

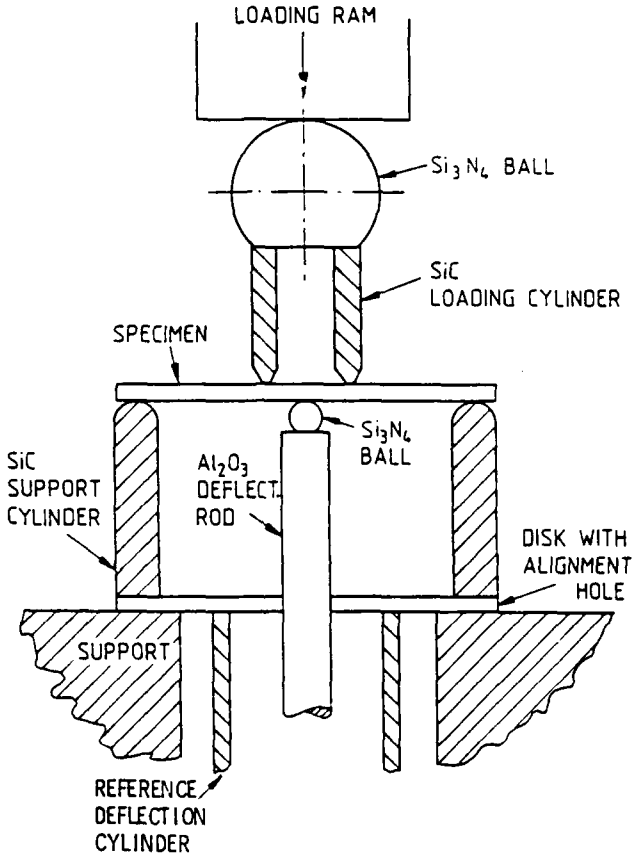

Figure 2. Schematic of the ring-on-ring equibiaxial fixtures.

Deflection was measured from the midpoint relative to the outer ring. A silicon nitride ball touched the specimen underside in order to ensure no contamination and a point contact. The outer ring and middle point deflections were transmitted to a linear voltage displacement transducer (LVDT) outside the furnace.

Stress rupture experiments were performed in a SiC resistance heating furnace equipped with a dead weight lever arm system.† The load was accurate to within 1%. Temperature was stabilized for 15 to 30 minutes prior to load application, which took 5 to 10 seconds.‡

*Crystar Grade, Norton Company.
†Netzsch High Temperature Flexure Strength Tester Model 422
‡The uniaxial specimens needed only 5 minutes to stabilize (Reference 10).

Temperature, which was held to within 3°C, was monitored by a platinum thermocouple located 2 mm above the specimen.

Six specimens were broken to determine a reference strength at room temperature. A screw-driven universal testing machine* was used at a crosshead rate of 0.5 mm/min causing failures in 20 to 30 seconds.

All stresses were computed from the elastic stress formula:[14-16]

$$\sigma = \frac{3P}{2\pi h^2} \left[(1-\upsilon)\ (a^2 - r^2) / 2b^2 + (1+\upsilon)\ \ln\ (\frac{a}{r}) \right]$$

where b is the specimen radius, a is the radius of the support ring, r is the load ring radius, h is the specimen thickness, and p is the load. Poisson's ratio, υ, was taken to be 0.26 at room temperature and 0.19 at 1200°C and 1300°C.[17]

The specimen and fixture sizes were chosen on the basis of the following criteria. First, it was desired to eliminate specimen size effects upon strength. The disks should have the same volume or area under maximum load, with a similar through-the-thickness stress gradient, so as to have similar Weibull effective surfaces or volumes. Secondly, since the loading rings were made of a refractory but weak ceramic, absolute load levels had to be kept low. Next, friction errors in loading, which could not entirely be eliminated (very difficult with high temperature fixtures), had to be comparable between the four-point and disk tests. Frictional constraint at the fixed load points can lead to errors of the order of 1% to 20% in stress in both four-point flexure[18] and biaxial disk testing.[15] In both cases, the friction error is directly proportional to the coefficient of friction (difficult to control at high temperature) and the specimen thickness. Giovan and Sines[19] minimized friction error in their low to moderate temperature ring-on-ring apparatus by the use of crowned loading rings and lapped specimens. Both steps were used in this study for the disks, however, since the coefficient of high temperature friction could not be controlled, the uniaxial and biaxial specimen thicknesses were kept similar so as to keep the parasitic friction moments comparable. Consideration of possible stress relaxations due to creep relaxation was a further motivation to use the same specimen thickness. These factors together led to a choice of disk thickness of 2.2 mm which is similar to the 2.1-mm or 2.3-mm flexure bar thicknesses used for the uniaxial stress rupture data base.[3,4]

The four-point spans had been of the order of 40 mm x 20 mm, but such dimensions for the ring diameters in biaxial loading would have required very high loads. Thus, an outer diameter of 40 mm was used, but with an inner diameter of 10 mm. The area in the inner ring which has constant stress is, thus, 79 mm^2 which is comparable to the 56-mm^2 and 71-mm^2 areas in the four-point specimens from the earlier studies.

*Instron Model 1195 Canton, MA, USA.

15. FESSLER, H., and FRICKER, D. C. *A Theoretical Analysis of the Ring-on-Ring Loading Disk Test.* J. Am. Ceram. Soc., v. 67, no. 9, 1984, p. 582-588.
16. RITTER, Jr., J. E., JAKUS, K., BATAKIS, A., and BANDYOPADHYAY, N. *Appraisal of Biaxial Strength Testing.* J. Non. Cryst. Solids, v. 38, 1980, p. 419-424.
17. KOSSOWSKY, R., MILLER, D. G., and DIAZ, E. S. *Tensile and Creep Strengths of Hot Pressed Si_3N_4.* J. Mat. Sci., v. 10, 1975, p. 983-997.
18. BARATTA, F. I., QUINN, G. D., and MATTHEWS, W. T. *Errors Associated with Flexure Testing of Brittle Materials.* U.S. Army Materials Technology Laboratory, MTL TR 87-35, July 1987.
19. GIOVAN, M. N., and SINES, G. *Strength of a Ceramic at High Temperatures Under Biaxial and Uniaxial Tension.* J. Am. Ceram. Soc., v. 64, no. 2, 1981, p. 68-73.

Finally, the error due to wedging stresses (due to excessive concentrated stresses under the loading ring) was minimized as a consequence of the system geometry. The absolute load to cause breakage was about ten times greater in the disk specimen, but the inner ring had six times more contact length, so the distributed load and, thus, the wedging stresses were comparable and rather low.

All of these preparations were successful as the fixtures were never damaged. The specimens broke in an ideal fashion, almost always within the middle gage area, and not under the load circle. So, in summary, the disk ring-on-ring test configuration is, in essence, a two-dimensional flexure test. As much as possible, testing conditions where chosen to permit a direct comparison to the one-dimensional, uniaxial flexure test.

RESULTS

The six disks broken at room temperature had an average strength of 501 MPa and a standard deviation of only ±29. A Weibull two-parameter analysis* gave a modulus of 19 (see Figure 3). Five of the fractures originated inside the gage area, and the sixth was outside the gage area. Figure 4 shows one of the former. Failure origins were readily observable based upon the crack branching patterns. Scanning electron microscopy, unfortunately, identified the strength limiting flaws in several specimens to be subsurface machining damage (see Figure 5a). Such damage appeared as 15 μm to 20 μm deep elongated semielliptical cracks which often overlapped. These occasionally intersected at different angles creating a zig-zag defect at the failure origin. This was possibly due to a shift in orientation of the specimen during surface grinding. Inclusions caused failure in at least one specimen. A mounting clay contamination problem obscured the origins in several specimens.

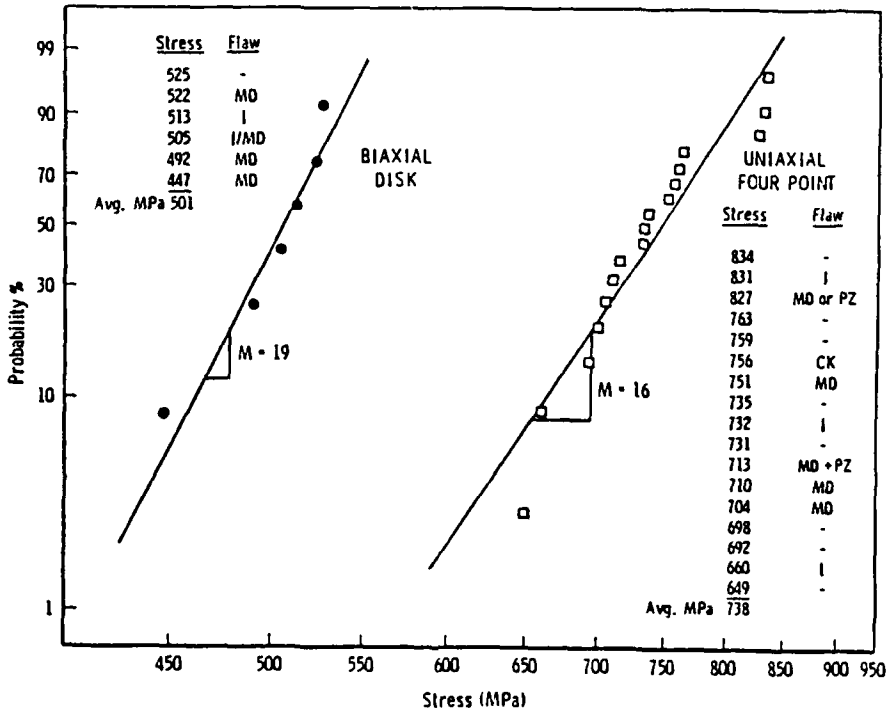

Figure 3. Room temperature uniaxial and biaxial strengths. In the flaw key, I denotes ar inclusion; MD, machining damage; PZ, a porous zone; CK, a crack; anc - is uncertain.

*Least squares analysis with probability of failure equal to (i-0.5)/n where i is the ith data point, and n is the total number of specimens.

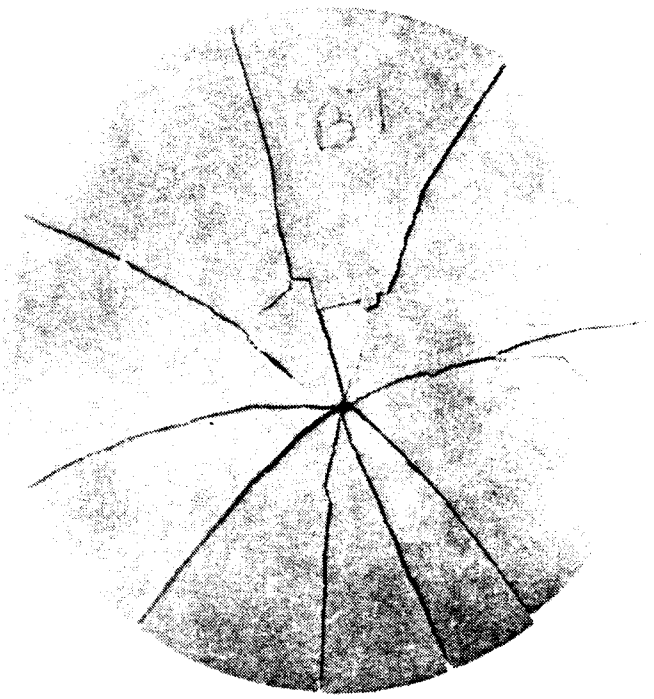

Figure 4. Disk specimen fracture at room temperature at 492 MPa. The arrow marks the failure origin.

The equibiaxial strength, 501 MPa, is substantially lower than the 738 MPa (±53 MPa) uniaxial strength which was measured on the 17 flexure bars. The uniaxial flexure, Weibull two-parameter modulus was 16 but could have been higher with the deletion of a few high strength points (see Figure 3). Strength limiting flaws, again, were either 15 μm to 25 μm deep semielliptical machining damage or tungsten inclusions. These inclusions typically were small broken-up particles (see Figures 5b and 5c). They were smaller than comparable strength penny-shaped defects, a consequence of a locally reduced fracture toughness.[12]

The stress rupture results at 1200°C are shown in Figure 6. Biaxial lifetimes appear to be considerably shortened but with high scatter relative to uniaxial stress rupture results (which are from References 2 to 4). Figures 7 and 8 show crack patterns in these specimens. The short duration specimens (<0.2 hour) had small intergranular slow crack growth (SCG) zones (100 μm to 500 μm) changing to a transgranular fast fracture crack. Longer-lived specimens had much larger crack growth zones. For example, the 250 MPa specimen at 0.4 hour had a 10-mm-long SCG region. Large SCG zones in four-point flexure are also possible,[11] but not as large as 10 mm. It must also be remembered that the uniform stress zone in the disk specimen is only 10 mm in diameter. Outside the inner loading ring the radial and tangential stresses diminish rapidly (the radial stresses the more so).[15,16]

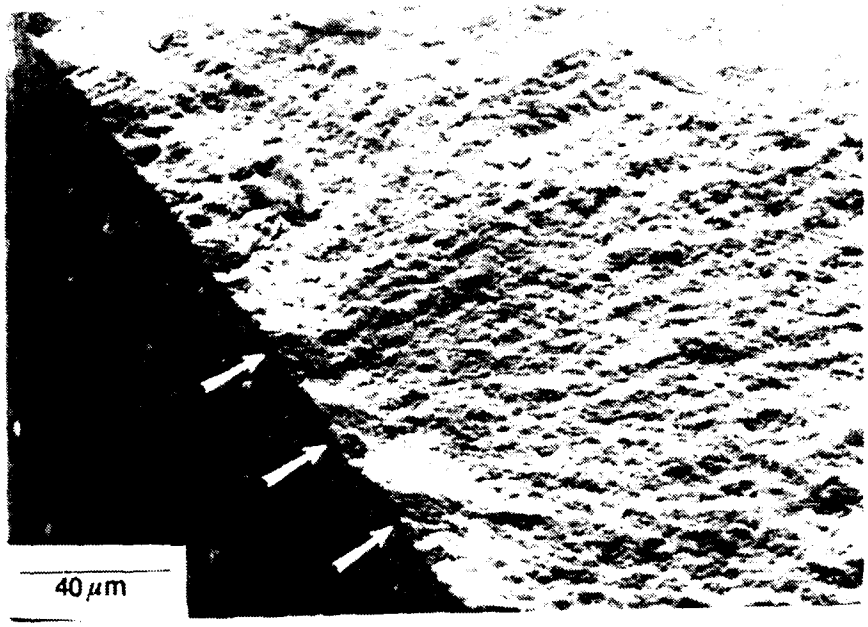

(a)

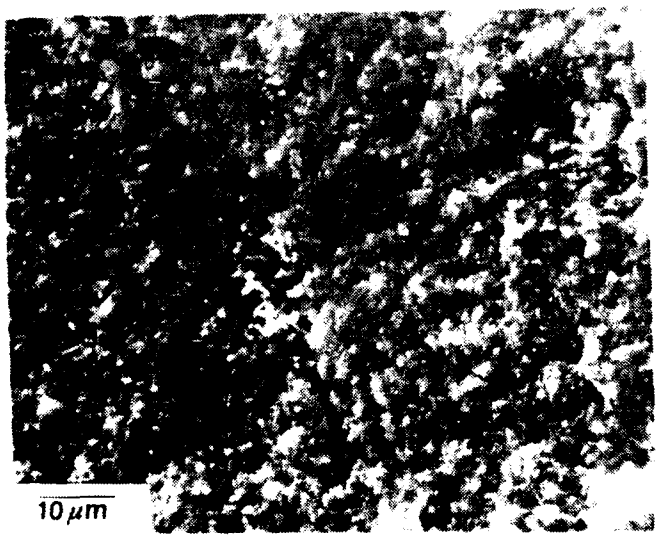

(b)

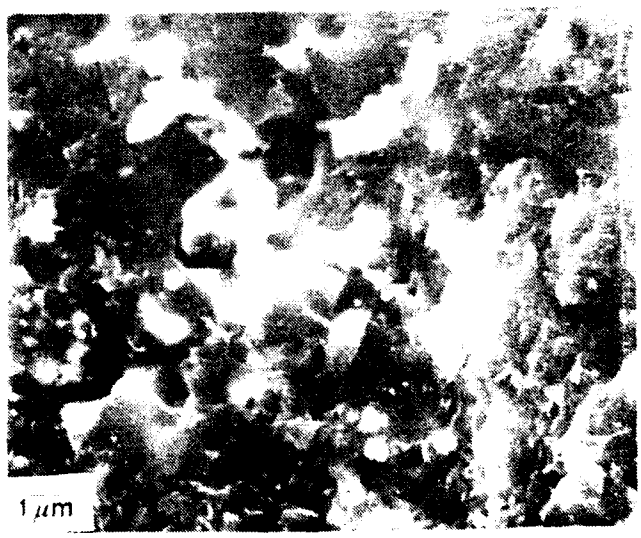

(c)

Figure 5. Fracture origin in disk and flexure specimens: (a) shows zig-zag machining damage as verified by radiating hackle (the particle in the upper left is a contaminant); (b) and C\(c) show a tungsten carbide or silicide inclusion.

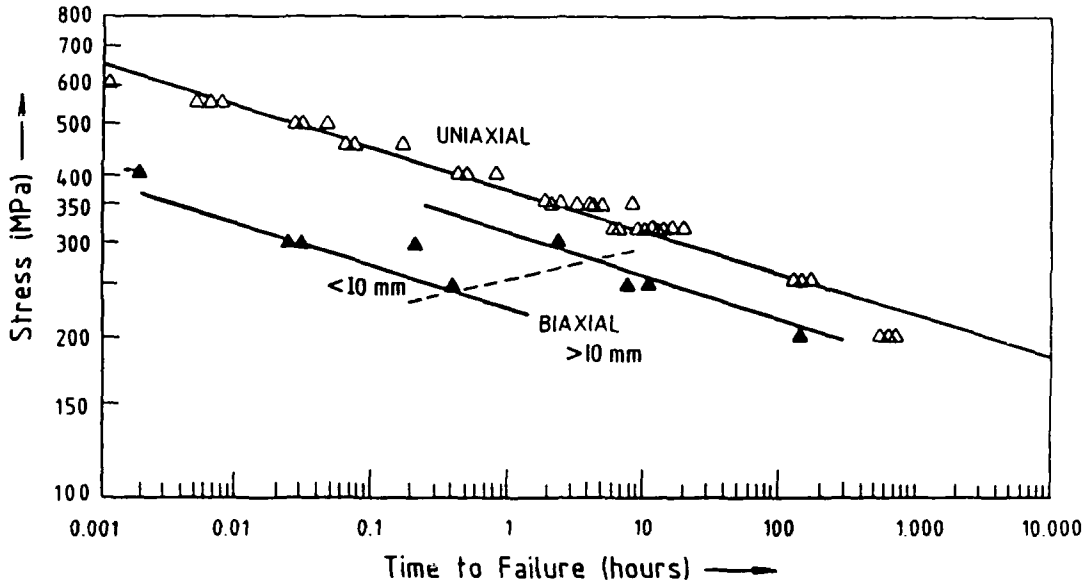

Figure 6. Biaxial stress rupture data (solid symbols) at 1200°C in air for HPSN. Uniaxial results (hollow points) are given for comparison (see References 3 and 10). The arrowed points are either failures on loading or an interrupted tests. The dashed line marks where SCG zones extended beyond the 10-mm central load region. The limits of the biaxial behavior are bounded by lines.

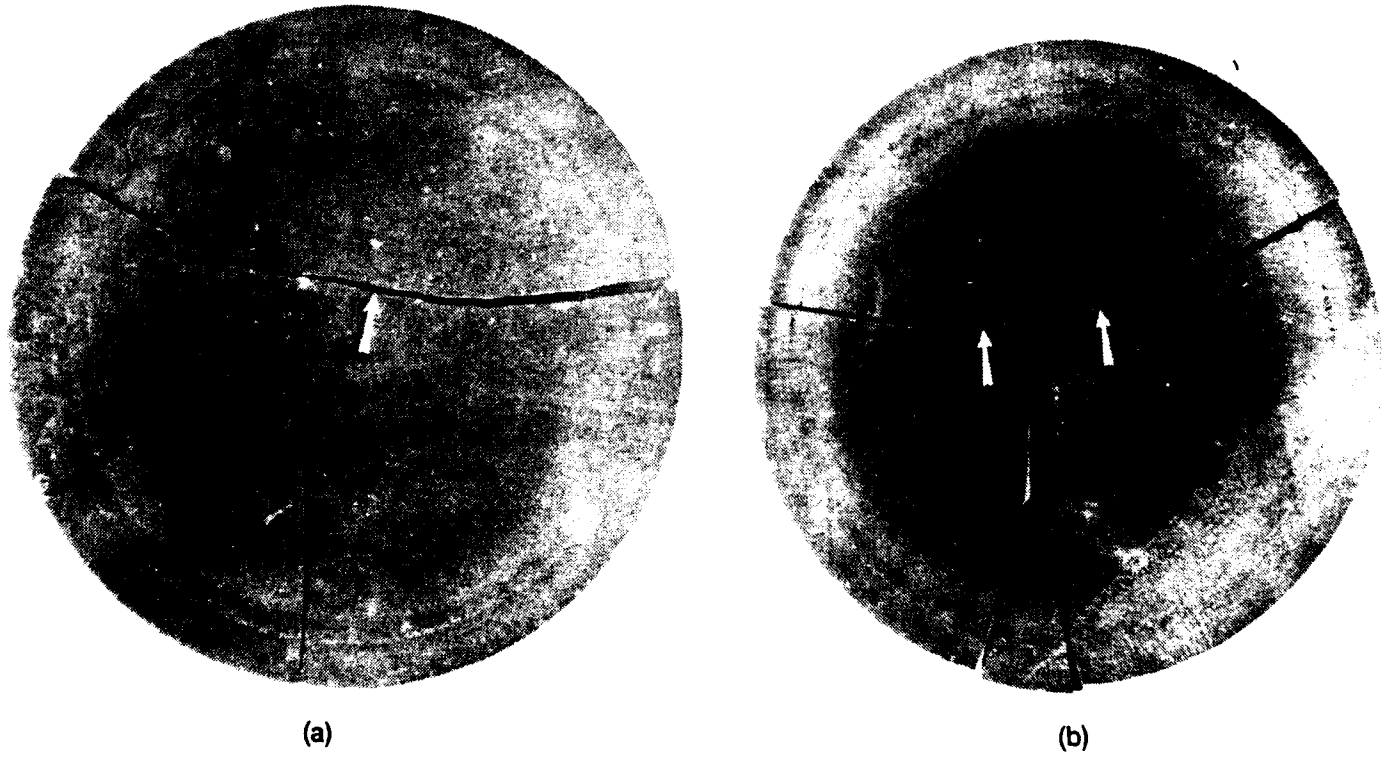

Figure 7. Disk stress rupture specimens: (a) specimen which failed at 1200°C after 0.2 hour with 300 MPa (the SCG zone was 1 mm long); (b) disk specimen that failed at 1200°C after 2.5 hours [the SCG zone was 8 mm long (arrows)].

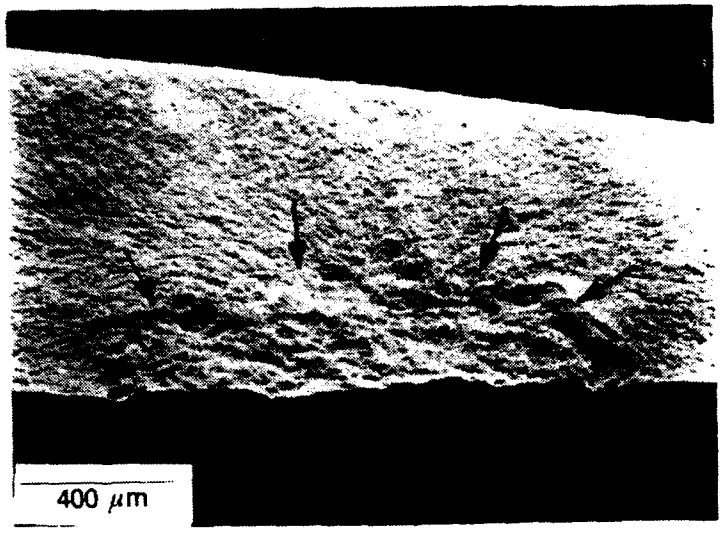

Figure 8. SEM photo of the fracture surface of the 1200°C specimen shown in Figure 7a.

The 1300°C biaxial results (see Figure 9) seem to be more clear since scatter in lifetime is dramatically reduced. Overall lifetime is shortened by a factor of about 20, but the static fatigue trend is comparable to the uniaxial results. The slope of a line through the biaxial results gives a SCG exponent of 8.4, whereas the uniaxial exponent is 9.9.* The SCG zones at 1300°C were much larger and more severe than at 1200°C. Even the short duration specimens had large zones of the order of 10 mm length which extended completely through the thickness. The specimens loaded at 200 MPa or less had SCG zones extending to the **outer** load ring, and even to the specimen rim. This is very unfortunate and it is clear that, with the exception of the first three specimens, the cracks in the specimen were typically moving through regions of nonuniform stress in the specimen. The last three specimen failures were due to creep fracture, and not slow crack growth as well.

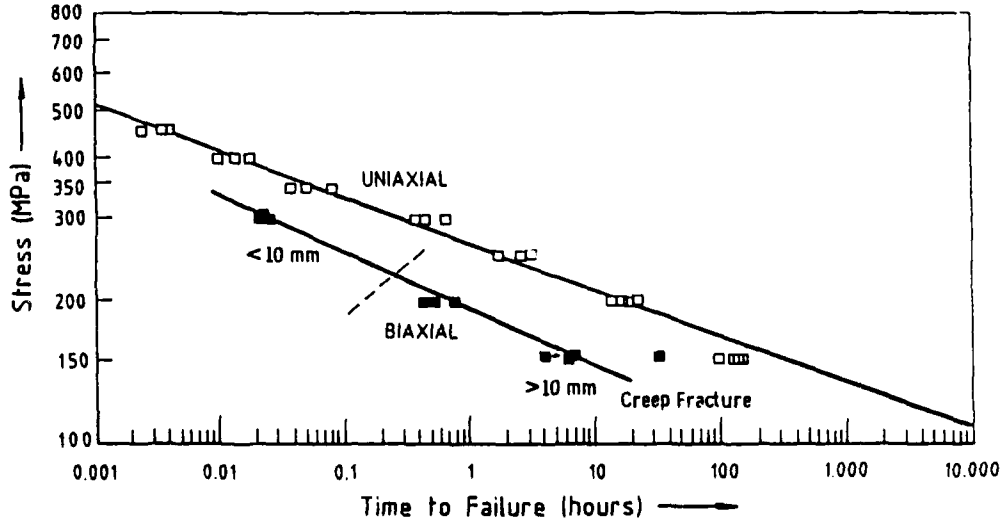

Figure 9. Biaxial stress rupture data at 1300°C in air (solid symbols). Uniaxial results (hollow symbols) are for comparison (see References 3 and 10). The dashed line marks the limit where SCG zones extended beyond the 10-mm central load region.

*Stress = constant x (time to failure)$^{-1/N}$ where N is the slow crack growth exponent (References 2 and 10).

DISCUSSION

It is disheartening to observe that after what apparently were careful precautions, machining damage persisted in both the bend bars and the disks. The machining damage was centered on, or exacerbated by, the presence of 1-μm to 3-μm sized pores in the materials, which is to say failure occurred from machining damage that may have interacted with natural microdefects. The zig zag, interactive machining damage in the disks would be formidable to analyze. Most previous studies, wherein machining damage was inferred as an interfering factor in disk specimens, did not actually verify it; e.g., Reference 14. In the present case, the machining vender, a reliable establishment, subcontracted the tedious lapping to another shop and the work was not done to specification. Only a few μm were removed, which produced a pretty 25 nm to 50 nm (1 to 2 rms microinch) surface, but only managed to conceal the subsurface cracks (15 μm to 20 μm). The 32% reduction in fast fracture strength from uniaxial to biaxial loading, therefore, has to be considered in the context of the statistics of machining damage variability (and not in the context of randomly oriented, noninteractive idealized defects). Most studies, both analytical and experimental, suggest equibiaxial weakening will be of the order of 5% to 20%*,[20-22] (although in a recent review, Rosenfield et al.* pointed out that there are several instances of biaxial strengthening in inert environments). Most all of these studies are clouded by experimental uncertainties (friction errors, uniaxial/biaxial size effects, or no fractography).

The reduction in stress rupture lifetime for biaxial loading is not surprising. The slow growth cracks followed a very tortuous and winding path at both 1200°C and 1300°C, and numerous multiple crack patterns, even cracks growing at directions normal to each other, were observed. The cracks seemed to be active in all directions. The irregularity of the cracks suggests extensive microcrack interactions, or, possibly, the ability to circumvent pockets of resistance. Such crack freedom was noted by Pletka and Wiederhorn in their comparison of uniaxial and biaxial crack growth behavior.[8] Although the biaxial lifetimes seem to be shorter, this may simply be a consequence of the dramatically reduced fast fracture strength (501 MPa) of the biaxial specimens. Indeed, if the data shown in Figures 6 and 9 are normalized by the reference strengths at room temperature, then the static fatigue curves are comparable and there is no biaxial lifetime shortening.†

The similarity in static fatigue strength degradation in biaxial and uniaxial modes of loading is reassuring since it would lead to simplified life prediction models. Service and Ritter[9] have also reported identical static fatigue susceptibilities in uniaxial or biaxial stress states. Pletka and Wiederhorn[7,8] showed consistent susceptibilities in uniaxial and biaxial disk strength testing as well.

The sanguine interpretations must be tempered by some serious experimental shortcomings, however. The first complicating factor is the large crack sizes in many of the biaxial specimens of the present study. These behaved, in many respects, like fracture mechanics specimens (such as double torsion). Double torsion experiments at 1200°C and 1300°C on

*ROSENFIELD, A. R., SHETTY, P. K., and DUCKWORTH, W. H. Strength of Ceramics Subjected to Biaxial Stresses: II Combined Normal Loads. Unpublished Research.

†The biaxial stress rupture results are normalized by the fast fracture data of this report (501 MPa). The uniaxial stress rupture data, if normalized by the fast fracture strength (738 MPa) of this report, will overlap. Alternatively, if the uniaxial strength from Reference 10 (909 MPa), where the flexure strength rupture results were originally reported is used, then the biaxial curve would actually shift higher than the uniaxial results. The fast fracture uniaxial results of Reference 10 were atypically high, as discussed.

20. WEIBULL, W. *Statistical Theory of the Strength of Materials*. Ingenioersvetenskapsakad. Handl., 1939., no. 151, p. 45.

21. BATDORF, S. D., and HEINISH, Jr., H. L. *Weakest Link Theory Reformulated for Arbitrary Fracture Criterion*. J. Am. Ceram. Soc., v. 61, no. 7-8, 1978, p. 355-358.

22. EVANS, A. G. *A General Approach for the Statistical Analysis of Multiaxial Fracture*. Idem., p. 302-308.

the identical material were reported previously by this author.[11] A striking similarity in the scatter of results was reported: high variability at 1200°C and good consistency at 1300°C. Variable zones of crack growth resistance were reported as well.[10] The crack fronts in the biaxial disk specimen (transition from SCG intergranular to fast fracture transgranular) were curved, much like fronts in double torsion specimens.

Whereas there was sufficient stored elastic energy in the biaxial fast fracture specimens to cause breakage once a flaw was critically loaded, this was **not** necessarily true in the stress rupture specimens which were loaded at much reduced levels. Thus, a crack which had grown from a few μm to 10 mm may have accelerated to velocities in the 10^{-3} to 10^{-2} m/sec range (which often is the highest practically measured velocities in static laboratory fracture mechanics tests), but then the crack could rapidly unload and decelerate as it reached the lower stressed region between the inner and outer rings. Any specimens where the crack growth markings extend much outside the inner ring, therefore, have to be regarded with skepticism. These are so noted in Figures 6 and 9. The fracture times can, at best, be considered overestimates.

The large cracks may have altered the specimen compliance, as shown in Figure 10. Indeed, it is peculiar consequence of the ring-on-ring system that, as a crack grows in one direction, the specimen will bend due to reduced compliance and, thus, will redistribute the ring loading to effectively reduce the stresses acting on the plane of the crack. Figure 10 shows that the loading rings will not evenly distribute the load as the specimen deflects preferentially in one direction.

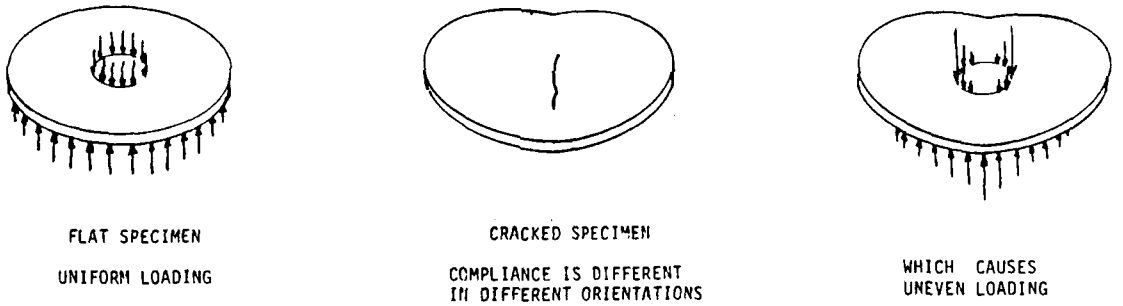

Figure 10. A cracked specimen has a nonuniform compliance which causes uneven loading.

Creep deformations are an additional complicating factor. Biaxial deformations often exhibited primary, secondary, and tertiary stages. The latter was, in the present case, undoubtedly due to a compliance effect as cracks became extremely large. Secondary creep deformation rates were never constant and always decreased, indicating no true steady state. Primary rates were as high as 100 times faster than minimum rates. Overall deflections were of the order of 0.1 mm to 1 mm for most specimens. The analysis of the deformation to give strains and relaxed stresses would be diabolically complicated. Several of these specimens were loaded in conditions of creep fracture. As an extreme example, the specimen loaded to 150 MPa at 1300°C was interrupted at 32 hours, as it was well into a tertiary creep deformation mode, but just a moment before fracture. It had numerous creep cracks and a central plug as almost punched out under the loading ring (see Figure 11).

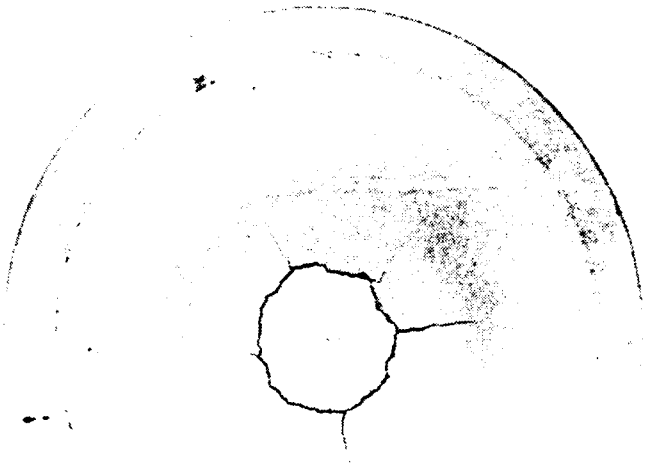

Figure 11. Specimen exhibiting excessive creep deformation and localized creep cracking at 32 hours at 1300°C with 150 MPa. The test was terminated just short of fracture when "tertiary" creep was well underway.

Finally, it was clear from the specimen fragments that creep and crack growth severely interfered with each other. That is, creep often blunted cracks and reduced stress intensities. Alternatively, crack growth created deformations that interfered with creep measurements.

CONCLUSIONS

1. The biaxial stress rupture lifetime of HPSN appears to be reduced compared to uniaxial lifetimes at high temperature. This is primarily due to a reduced fast fracture strength.

2. The biaxial fatigue trend of strength degradation appears to be the same as the uniaxial trend.

3. Biaxial SCG cracks wend a tortuous path through the specimen, unlike biaxial fast fracture or uniaxial cracks.

4. The fast fracture strength-limiting defects were the same in the biaxial and uniaxial specimens: machining damage and tungsten carbide or silicide inclusions.

5. The machining damage persisted despite careful specifications intended to remove it. The very pessimistic conclusions of Giovan and Sines[14] regarding machining damage should be addended to include: "Careful specifications will not guarantee proper specimen preparation."

6. The ring-loaded disk specimen exhibited a wide range of behavior. Some fractures were ideal strength (i.e., small crack, no creep) type specimens, others were like fracture

mechanics (large crack) specimens, and finally, some as creep fracture specimens. There was a tendency for stresses to redistribute as the compliance changed due to large crack growth.

7. The ring-loaded disk specimen should only be used for stress rupture experiments where crack sizes and deformations are small.

ACKNOWLEDGMENT

The principle author wishes to thank Dr. R. N. Katz of the U.S. Army Material Technology Laboratory who suggested these experiments. The assistance of Mr. Bernd Kanka of DLR and Ms. Gail Meyers of MTL with scanning electron microscopy is appreciated.

DISTRIBUTION LIST

No. of Copies	To
1	Office of the Under Secretary of Defense for Research and Engineering, The Pentagon, Washington, DC 20301
	Commander, U.S. Army Laboratory Command, 2800 Powder Mill Road, Adelphi, MD 20783-1145
1	ATTN: AMSLC-IM-TL
1	AMSLC-CT
	Commander, Defense Technical Information Center, Cameron Station, Building 5, 5010 Duke Street, Alexandria, VA 22304-6145
2	ATTN: DTIC-FDAC
1	Metals and Ceramics Information Center, Battelle Columbus Laboratories, 505 King Avenue, Columbus, OH 43201
	Commander, Army Research Office, P.O. Box 12211, Research Triangle Park, NC 27709-2211
1	ATTN: Information Processing Office
	Commander, U.S. Army Materiel Command, 5001 Eisenhower Avenue, Alexandria, VA 22333
1	ATTN: AMCLD
	Commander, U.S. Army Materiel Systems Analysis Activity, Aberdeen Proving Ground, MD 21005
1	ATTN: AMXSY-MP, H. Cohen
	Commander, U.S. Army Missile Command, Redstone Scientific Information Center, Redstone Arsenal, AL 35898-5241
1	ATTN: AMSMI-RD-CS-R/Doc
1	AMSMI-RLM
	Commander, U.S. Army Armament, Munitions and Chemical Command, Dover, NJ 07801
2	ATTN: Technical Library
1	AMDAR-LCA, Mr. Harry E. Pebly, Jr., PLASTEC, Director
	Commander, U.S. Army Natick Research, Development and Engineering Center, Natick, MA 01760
1	ATTN: Technical Library
	Commander, U.S. Army Satellite Communications Agency, Fort Monmouth, NJ 07703
1	ATTN: Technical Document Center
	Commander, U.S. Army Tank-Automotive Command, Warren, MI 48397-5000
1	ATTN: AMSTA-ZSK
2	AMSTA-TSL, Technical Library
	Commander, White Sands Missile Range, NM 88002
1	ATTN: STEWS-WS-VT
	President, Airborne, Electronics and Special Warfare Board, Fort Bragg, NC 28307
1	ATTN: Library
	Director, U.S. Army Ballistic Research Laboratory, Aberdeen Proving Ground, MD 21005
1	ATTN: SLCBR-TSB-S (STINFO)
	Commander, Dugway Proving Ground, Dugway, UT 84022
1	ATTN: Technical Library, Technical Information Division
	Commander, Harry Diamond Laboratories, 2800 Powder Mill Road, Adelphi, MD 20783
1	ATTN: Technical Information Office
	Director, Benet Weapons Laboratory, LCWSL, USA AMCCOM, Watervliet, NY 12189
1	ATTN: AMSMC-LCB-TL
1	AMSMC-LCB-R
1	AMSMC-LCB-RM
1	AMSMC-LCB-RP
	Commander, U.S. Army Foreign Science and Technology Center, 220 7th Street, N.E., Charlottesville, VA 22901
1	ATTN: Military Tech

No. of Copies	To
	Commander, U.S. Army Aeromedical Research Unit, P.O. Box 577, Fort Rucker, AL 36360
1	ATTN: Technical Library
	Commander, U.S. Army Aviation Systems Command, Aviation Research and Technology Activity, Aviation Applied Technology Directorate, Fort Eustis, VA 23604-5577
1	ATTN: SAVDL-E-MOS
	U.S. Army Aviation Training Library, Fort Rucker, AL 36360
1	ATTN: Building 5906-5907
	Commander, U.S. Army Agency for Aviation Safety, Fort Rucker, AL 36362
1	ATTN: Technical Library
	Commander, USACDC Air Defense Agency, Fort Bliss, TX 79916
1	ATTN: Technical Library
	Commander, U.S. Army Engineer School, Fort Belvoir, VA 22060
1	ATTN: Library
	Commander, U.S. Army Engineer Waterways Experiment Station, P. O. Box 631, Vicksburg, MS 39180
1	ATTN: Research Center Library
	Commandant, U.S. Army Quartermaster School, Fort Lee, VA 23801
1	ATTN: Quartermaster School Library
	Naval Research Laboratory, Washington, DC 20375
1	ATTN: Code 5830
2	Dr. G. R. Yoder - Code 6384
	Chief of Naval Research, Arlington, VA 22217
1	ATTN: Code 471
1	Edward J. Morrissey, AFWAL/MLTE, Wright-Patterson Air Force, Base, OH 45433
	Commander, U.S. Air Force Wright Aeronautical Laboratories, Wright-Patterson Air Force Base, OH 45433
1	ATTN: AFWAL/MLC
1	AFWAL/MLLP, M. Forney, Jr.
1	AFWAL/MLBC, Mr. Stanley Schulman
	National Aeronautics and Space Administration, Marshall Space Flight Center, Huntsville, AL 35812
1	ATTN: R. J. Schwinghammer, EH01, Dir, M&P Lab
1	Mr. W. A. Wilson, EH41, Bldg. 4612
	U.S. Department of Commerce, National Institute of Standards and Technology, Gaithersburg, MD 20899
1	ATTN: Stephen M. Hsu, Chief, Ceramics Division, Institute for Materials Science and Engineering
1	Committee on Marine Structures, Marine Board, National Research Council, 2101 Constitution Ave., N.W., Washington, DC 20418
1	Librarian, Materials Sciences Corporation, Guynedd Plaza 11, Bethlehem Pike, Spring House, PA 19477
1	The Charles Stark Draper Laboratory, 68 Albany Street, Cambridge, MA 02139
	Wyman-Gordon Company, Worcester, MA 01601
1	ATTN: Technical Library
	Lockheed-Georgia Company, 86 South Cobb Drive, Marietta, GA 30063
1	ATTN: Materials and Processes Engineering Dept. 71-11, Zone 54
	General Dynamics, Convair Aerospace Division, P.O. Box 748, Fort Worth, TX 76101
1	ATTN: Mfg. Engineering Technical Library
1	Mechanical Properties Data Center, Belfour Stulen Inc., 13917 W. Bay Shore Drive, Traverse City, MI 49684
	Director, U.S. Army Materials Technology Laboratory, Watertown, MA 02172-0001
2	ATTN: SLCMT-TML
2	Authors

U.S. Army Materials Technology Laboratory
Watertown, Massachusetts 02172-0001
BIAXIAL STRENGTH STRESS RUPTURE
OF HOT-PRESSED SILICON NITRIDE -
George D. Quinn and Gunter Wirth

AD________________
UNCLASSIFIED
UNLIMITED DISTRIBUTION

Key Words

Silicon nitride
Static fatigue life
Disk testing

Technical Report MTL TR 89-101, November 1989, 16 pp-
illustrations, D/A Project: 1L1612105.AH84

The equibiaxial static fatigue resistance of hot-pressed silicon nitride was measured at high temperature. A concentric ring scheme was used to load disks at up to 1300°C in air. Equibiaxial lifetimes were substantially shorter than uniaxial lifetimes, primarily a consequence of a drastically reduced biaxial strength. The static fatigue trends were similar in uniaxial and biaxial loading. The ring-on-ring scheme is not suitable for stress rupture testing if creep deformations are present or cracks grow large without going critical.

U.S. Army Materials Technology Laboratory
Watertown, Massachusetts 02172-0001
BIAXIAL STRENGTH STRESS RUPTURE
OF HOT-PRESSED SILICON NITRIDE -
George D. Quinn and Gunter Wirth

AD________________
UNCLASSIFIED
UNLIMITED DISTRIBUTION

Key Words

Silicon nitride
Static fatigue life
Disk testing

Technical Report MTL TR 89-101, November 1989, 16 pp-
illustrations, D/A Project: 1L1612105.AH84

The equibiaxial static fatigue resistance of hot-pressed silicon nitride was measured at high temperature. A concentric ring scheme was used to load disks at up to 1300°C in air. Equibiaxial lifetimes were substantially shorter than uniaxial lifetimes, primarily a consequence of a drastically reduced biaxial strength. The static fatigue trends were similar in uniaxial and biaxial loading. The ring-on-ring scheme is not suitable for stress rupture testing if creep deformations are present or cracks grow large without going critical.

U.S. Army Materials Technology Laboratory
Watertown, Massachusetts 02172-0001
BIAXIAL STRENGTH STRESS RUPTURE
OF HOT-PRESSED SILICON NITRIDE -
George D. Quinn and Gunter Wirth

AD________________
UNCLASSIFIED
UNLIMITED DISTRIBUTION

Key Words

Silicon nitride
Static fatigue life
Disk testing

Technical Report MTL TR 89-101, November 1989, 16 pp-
illustrations, D/A Project: 1L1612105.AH84

The equibiaxial static fatigue resistance of hot-pressed silicon nitride was measured at high temperature. A concentric ring scheme was used to load disks at up to 1300°C in air. Equibiaxial lifetimes were substantially shorter than uniaxial lifetimes, primarily a consequence of a drastically reduced biaxial strength. The static fatigue trends were similar in uniaxial and biaxial loading. The ring-on-ring scheme is not suitable for stress rupture testing if creep deformations are present or cracks grow large without going critical.

U.S. Army Materials Technology Laboratory
Watertown, Massachusetts 02172-0001
BIAXIAL STRENGTH STRESS RUPTURE
OF HOT-PRESSED SILICON NITRIDE -
George D. Quinn and Gunter Wirth

AD________________
UNCLASSIFIED
UNLIMITED DISTRIBUTION

Key Words

Silicon nitride
Static fatigue life
Disk testing

Technical Report MTL TR 89-101, November 1989, 16 pp-
illustrations, D/A Project: 1L1612105.AH84

The equibiaxial static fatigue resistance of hot-pressed silicon nitride was measured at high temperature. A concentric ring scheme was used to load disks at up to 1300°C in air. Equibiaxial lifetimes were substantially shorter than uniaxial lifetimes, primarily a consequence of a drastically reduced biaxial strength. The static fatigue trends were similar in uniaxial and biaxial loading. The ring-on-ring scheme is not suitable for stress rupture testing if creep deformations are present or cracks grow large without going critical.